

Emergence of one-dimensional physics from the distorted Shastry-Sutherland lattice

M. Moliner,^{1,*} I. Rousochatzakis,^{2,†} and F. Mila^{3,‡}

¹*Institut für Nanotechnologie, Karlsruhe Institute of Technology, D-76344 Eggenstein-Leopoldshafen, Germany*

²*Max-Planck-Institut für Physik komplexer Systeme, Nötnitzer Straße 38, D-01187 Dresden, Germany*

³*Institute of Theoretical Physics, Ecole Polytechnique Fédérale de Lausanne, CH-1015 Lausanne, Switzerland*

(Received 23 December 2010; revised manuscript received 25 March 2011; published 28 April 2011)

Motivated by the ongoing investigation of $\text{SrCu}_2(\text{BO}_3)_2$ under pressure, we study a variant of the two-dimensional Shastry-Sutherland (SS) spin-1/2 model with two types of dimers. Combined with the frustration of the SS model, this modification induces, in a large parameter range, a dimensional reduction at low energies, with nearly decoupled effective $S = 1$ Haldane chains forming along one of the diagonals of the lattice. We also present evidence that the intermediate plaquette solid phase of the undistorted SS model remains stable in a finite region of the phase diagram.

DOI: [10.1103/PhysRevB.83.140414](https://doi.org/10.1103/PhysRevB.83.140414)

PACS number(s): 75.10.Jm, 75.10.Kt, 75.30.Kz

Introduction. An exciting route for exploring new phases in frustrated magnets consists of applying hydrostatic pressure so as to considerably modify the dominant magnetic interactions and thus alter the relevant low-energy degrees of freedom. The quasi-two-dimensional (quasi-2D) compound $\text{SrCu}_2(\text{BO}_3)_2$ ¹ offers such a possibility since it is in the close vicinity of a quantum phase transition from an exact tensor product of singlets toward a plaquette solid.^{2,3} Indeed, nuclear magnetic resonance (NMR),^{4,5} inelastic neutron scattering (INS),⁶ as well as earlier susceptibility measurements,⁷ show strong evidence that $\text{SrCu}_2(\text{BO}_3)_2$ undergoes at least one phase transition under high hydrostatic pressure, the nature of which is still not fully understood. What is clear, however, is that the fourfold (C_4) symmetry around the void plaquettes is quickly lost under pressure, so that nearest-neighbor dimers pointing in different directions become inequivalent (see Fig. 1). This naturally leads to an extension of the Shastry-Sutherland (SS) model with two different diagonal bonds J_1 and J_2 described by the spin $S = 1/2$ Heisenberg Hamiltonian,

$$\mathcal{H} = J' \sum_{\langle ij \rangle} \mathbf{S}_i \cdot \mathbf{S}_j + J_1 \sum_{\langle\langle ij \rangle\rangle_1} \mathbf{S}_i \cdot \mathbf{S}_j + J_2 \sum_{\langle\langle ij \rangle\rangle_2} \mathbf{S}_i \cdot \mathbf{S}_j, \quad (1)$$

where J' denotes the nearest-neighbor exchange (see Fig. 1). Since all nearest-neighbor bonds J' are equal, the product of singlets on J_1 and J_2 bonds is always an eigenstate, as it is for the undistorted SS model. Besides, although the C_4 symmetry is lost, both the sets of J_1 and J_2 bonds form a square lattice. It thus seems natural to expect that the phase diagram will consist of three phases, as for the regular SS model: the exact singlet phase for small J' , the Néel phase for large J' , and an intermediate plaquette phase with 2D character.^{2,3}

In this Rapid Communication, using a variety of analytical and numerical techniques, we show that making the diagonal bonds inequivalent actually triggers an abrupt dimensional reduction into an effectively 1D Haldane phase in a wide parameter range (see Fig. 2). In this phase the effective low-energy physics can be described in terms of nearly decoupled, fully frustrated two-leg ladders (see Fig. 1) running along one of the two diagonals of the square lattice. Remarkably enough, the spins on the J_2 bonds form *triplets* in this phase, leading to a completely different picture of the low-lying magnetic excitations as compared to the exact singlet phase.

The emergence of this new singlet phase is best understood by starting from the limit $J_2/J_1 = J'/J_1 = 0$. The model then reduces to a set of isolated dimers on the J_1 bonds and isolated free spins on the remaining sites (see Fig. 1), resulting in a macroscopically degenerate ground-state manifold. The degeneracy is lifted by switching on the interdimer coupling J' which, to leading (second) order, *a priori* couples a given spin to 12 neighbors (see Fig. 1, where the 12 neighbors of site 0 are numbered from 1 to 12). Each second-order process involves an intermediate state with a J_1 dimer in a triplet state, and the resulting coupling is ferromagnetic and of amplitude $-J'^2/2J_1$ if the J' bonds are connected to the same site of the J_1 dimer, while it is antiferromagnetic and of amplitude $J'^2/2J_1$ if they are connected to opposite sites. When processes with different signs couple two spins, they cancel out due to quantum interferences. As a result, the couplings between site 0 and sites 6 to 12 vanish, and site 0 is only coupled to its neighbors on the ladder shown in Fig. 1. The couplings between site 0 and sites 2, 3, 4, and 5 are all antiferromagnetic

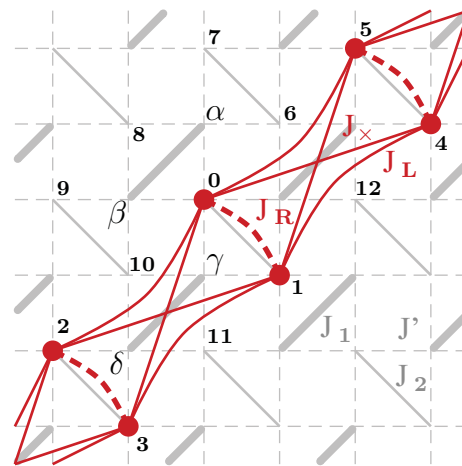


FIG. 1. (Color online) The distorted SS model (thick and thin gray lines for J_1 , J_2 , respectively, and dashed for J') of this work, together with the effective quasi-1D model (red solid and dashed thick lines) emerging in the limit $J_1 \gg J_2, J'$, which gives rise to the Haldane phase.

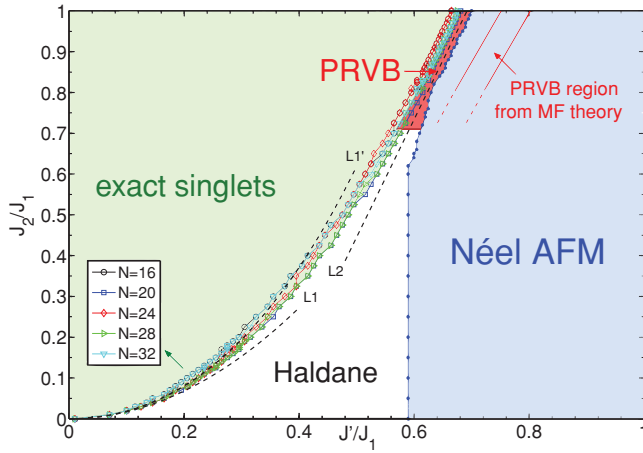


FIG. 2. (Color online) The phase diagram of the present model as obtained by exact diagonalizations (symbols with lines). The red lines enclose the stability region of the PRVB phase as obtained from the quadrumer boson operator method (see text). The dashed lines L1 and L1' denote the boundary between the exact dimer and the Haldane phase as obtained from perturbation theory up to second and third orders, while the dashed line L2 is the line along which we examine the low-E spectrum shown in Fig. 5 below.

and of amplitude $J^2/2J_1$, while the coupling between 0 and 1 is ferromagnetic and equal to $-J^2/J_1$.

Including both J_2 and J' , and up to second order in J'/J_1 , our 2D model thus reduces to an infinite set of two-leg, frustrated spin ladders directed along the J_1 diagonal bonds. The effective interactions within the ladders are depicted in Fig. 1 on top of the original model. They consist of the rung coupling $J_R = J_2 - J^2/J_1$, the leg coupling $J_L = J^2/2J_1$, and a frustrating coupling $J_x = J_L$. This model has been studied quite extensively.^{8,9} It has the special property that the total spin on each rung is a good quantum number, which makes it possible to determine a large number of eigenstates exactly.⁸ In particular, in the limit $J_R \gg J_L$ (or $J_2 \gg J^2/J_1$) the lowest energy is obtained by minimizing the number of triplets in the rungs.¹⁰ The resulting ground state of the ladder is the product of rung singlets, which together with the strong J_1 singlets correspond to the exact orthogonal-dimer phase of the SS model. On the contrary, if J_R is not too large (and *a fortiori* if it is negative), fluctuations between neighboring triplets dominate and the lowest energy is obtained by placing a triplet on each rung. The ladder then behaves like a spin-1 chain, and hence the ground state corresponds to the Haldane gapped phase.¹¹ The actual transition between the exact dimer and the Haldane phase is known⁸ to take place at $J_R/J_L \simeq 1.4$ and it is of first order. Rewritten in terms of the original couplings of our model, this boundary corresponds to the line $J_2 = 1.7 J^2/J_1$, which is shown by the dashed line L1 in Fig. 2. The dashed line L1', defined by $J_2 = 1.7 J^2/J_1 + 1.55 J^3/J_1^2$, corresponds to the boundary obtained from perturbation theory up to third order.¹² Third-order processes in J'/J_1 also induce some coupling between nearest and next-to-nearest neighboring ladders, resulting in a complex network,¹³ but the quasi-1D character of the (short-range) spin correlations and the finite spin gap seem to be a robust feature of this phase, as suggested by exact diagonalizations.

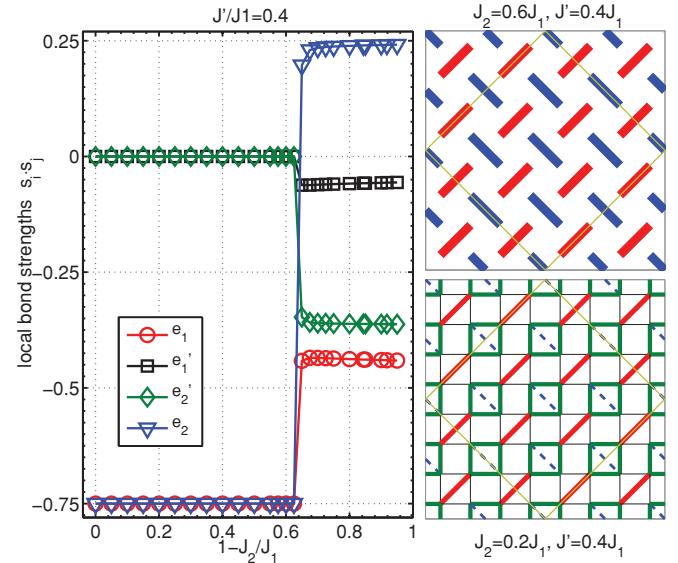


FIG. 3. (Color online) (Left panel) Ground-state expectation values of the four different nearest-neighbor exchange energies $\mathbf{S}_i \cdot \mathbf{S}_j$ for the 32-site cluster ($e_{1,2}$ for the $J_{1,2}$ diagonal bonds, and $e'_{1,2}$ for J' bonds on plaquettes which contain $J_{1,2}$ bonds). (Right panels) The corresponding local energy profiles for representative cases inside the exact singlet state (above) and the Haldane state (below). Positive (negative) exchange values are shown by dashed (solid) lines, whose width is proportional to the magnitude of these values.

Exact diagonalizations. To determine the behavior of the present model away from the above perturbative regime and to accurately obtain the full phase diagram of the model, we have performed an extensive exact diagonalization (ED) study on finite-size clusters with periodic boundary conditions. Apart from U(1) spin rotations and translational invariance we have also exploited the two reflection symmetries (denoted here by \mathcal{R}_1 and \mathcal{R}_2) along the two diagonals of the square lattice.

The transition between the exact singlet phase and the Haldane phase is most simply identified by measuring the ground-state spin-spin correlations $\langle \mathbf{S}_i \cdot \mathbf{S}_j \rangle$ on neighboring bonds, as shown in Fig. 3: They are rigorously equal to $-3/4$ on dimer bonds and to zero on J' bonds in the exact dimer phase and jump upon entering the Haldane phase to ferromagnetic and nearly equal to $1/4$ on the J_2 bonds and to intermediate antiferromagnetic values on J_1 and J' bonds. The resulting first-order transition lines shown in Fig. 2 are in good agreement with the perturbative predictions and show a weak system size dependence. In addition, the correlation profiles shown in the right panels of Fig. 3 demonstrate how the 2D lattice decouples into almost noninteracting two-leg ladders.

Next, we examine the behavior of the spin gap by looking at the evolution of the low-energy excitation spectrum as we move away from the exact dimer into the Haldane phase. Figure 4 shows the low-energy spectrum of the 32-site cluster along the line $J' = 0.4J_1$ in the $S_z = 0$ and 1 sectors. All energies are measured from the ground state. In the exact dimer phase the spin gap scales linearly with J_2 and thus decreases as we go toward the Haldane phase. This happens because a magnetic $S = 1$ excitation results by promoting a rung

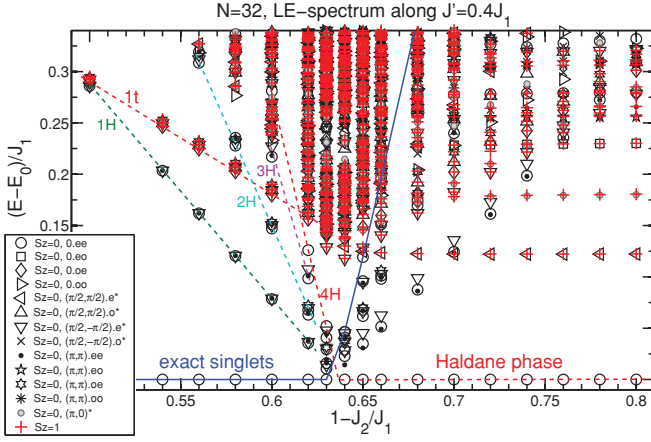


FIG. 4. (Color online) Low-energy spectrum (measured from the ground state) for the 32-site cluster along the line $J'/J_1 = 0.4$ in the $S_z = 0$ and 1 sectors. The blue solid line shows the energy of the exact singlet phase. The dashed lines highlight the n -Haldane chain singlets discussed in the text. The quantum numbers shown in the legends correspond to the allowed momenta of the 32-site cluster and the parities with respect to the two diagonal reflections $\mathcal{R}_{1,2}$.

singlet¹⁴ into a triplet, which costs energy J_2 [disregarding the polarization corrections to the spin gap driven by J' (Ref. 1)]. By contrast, when entering the Haldane phase at $J_2 \simeq 0.365J_1$ the gap does not change with J_2 any longer. This happens because once we pay the energy to form the effective spin-1 entities on the rungs the energy scale J_2 does not enter their effective dynamics any longer.

The 1D character of the Haldane phase underlies also a number of striking spectral features in the singlet sector. In particular, Fig. 4 shows a number of singlets (highlighted by dashed lines) which group together into almost degenerate levels, and all seem to become soft together with the Haldane state (red dashed line). These correspond to singlets where not all ladders are in the Haldane phase. Specifically, the 32-site cluster (enclosed by solid yellow lines in the right panels of Fig. 3) decomposes into four two-leg ladders with two J_2 bonds each. To form the Haldane phase in a single ladder we pay energy $2J_2$ to create two triplets (disregarding again the polarization energy driven by J'), but we gain an energy δ_H from their interaction. This gives four possible states with energy $E_{1H} \simeq 2J_2 - \delta_H$, whereby one ladder has entered the Haldane phase but the remaining three have still singlets in their rungs. Similarly, there must exist six states with two ladders in the Haldane phase and energy $E_{2H} \simeq 2E_{1H}$, four states with three ladders in the Haldane phase and $E_{3H} \simeq 3E_{1H}$, and finally a single state where all ladders are in the Haldane phase with $E_{4H} \simeq 4E_{1H}$. Both the multiplicities and the dependence on J_2 (the slope in the dashed lines of Fig. 4) are in agreement with the ED spectra. In addition, we have derived the decomposition of each group of singlets into irreducible representations of the space group of the 32-site cluster and the results also agree with the ED spectra. Finally, the fact that $E_{nH} \simeq nE_{1H}$ explains why the above groups of singlets seem to become soft together with the Haldane state.

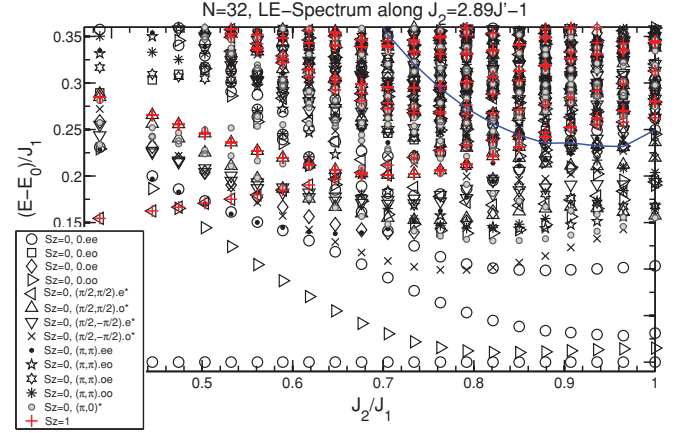


FIG. 5. (Color online) Low-energy spectrum (measured from the ground state) of the 32-site cluster along the line L_2 ($J_2 = 2.89J' - 1$) of Fig. 2 in the $S_z = 0$ and 1 sectors. The solid (blue) line stands for the energy of the exact singlet phase.

We note here that the above energy considerations are only true to leading order in J' . There are various perturbative corrections which renormalize the energy of each of the above singlets in a different manner. For the 32-site cluster, it is the global Haldane state that crosses the exact singlet phase first.

Upon increasing J'/J_1 , the Haldane phase undergoes a second-order transition into the Néel phase. The disappearance of the Néel order is continuous and corresponds to the vanishing of the local moment m obtained by a usual³ finite-size extrapolation $m_N \simeq m + \frac{c}{\sqrt{N}}$, using numerical data for the corresponding spin structure factor at zero momentum.¹⁵ We find that for $J_2 \lesssim 0.6J_1$, the Néel boundary does not depend on J_2 , which is related to the absence of this energy scale from the effective dynamics of the Haldane phase. On the other hand, the bending of the Néel boundary for $J_2 \gtrsim 0.6J_1$ indicates the proximity to another phase, different from the Haldane one. We now show evidence, first by a detailed spectral analysis and then by a perturbative mean-field approach, that this phase is adiabatically connected to the plaquette phase present for $J_2 = J_1$.^{2,3} We begin by examining the evolution of the low-lying spectrum along the line L_2 of Fig. 2. As shown in Fig. 5 for the 32-site spectrum, a low-energy excitation becomes gradually soft above $J_2/J_1 \sim 0.7-0.8$. This excitation has zero momentum but it has odd parity with respect to \mathcal{R}_1 and \mathcal{R}_2 , in contrast to the ground state. If these two states become degenerate in the thermodynamic limit, then the above quantum numbers are exactly the ones expected for the Z_2 plaquette phase, since the latter does not break translational invariance but it does break \mathcal{R}_1 and \mathcal{R}_2 .

We also find a large number of singlets below the lowest triplet excitation. The majority of these states have a positive curvature with J_2 , similarly to the exact singlet state shown by the solid (blue) line. Hence, these states are most probably adiabatically connected to singlets above the dimer phase, such as the ones we discussed above that must become nearly soft at the boundary with the Haldane phase (in addition, there could also be some bound states of triplons¹⁶). In agreement with Läuchli *et al.*,³ we also find a singlet which lies slightly above

the lowest two singlets at $J_2 = J_1$. The nature of this singlet might well be a singlet excitation (e.g., a domain wall) of the plaquette phase.

A complementary confirmation that the plaquette phase survives in a small region for $J_2 \neq J_1$ can be also given by an analytical mean-field approach based on quadrumer boson operators.^{3,17–19} Here one essentially expands around the explicitly symmetry broken phase where every second void square is in the singlet ground state of an isolated Heisenberg plaquette.² The ground-state and low-lying excitations of the original model are then approximated by truncating the Hilbert space of each plaquette to its singlet ground state and its lowest triplet, which is achieved by the bosonic representation of the four spins ($j = 1, \dots, 4$),

$$S_j^\alpha = \frac{(-1)^j}{\sqrt{6}}(s^\dagger t_\alpha + t_{\alpha s}^\dagger) - \frac{i}{4} \sum_{\beta, \gamma} \epsilon^{\alpha\beta\gamma} t_\beta^\dagger t_\gamma, \quad (2)$$

where $\alpha = x, y, z$, and $s^\dagger, t_\alpha^\dagger$ create, respectively, the singlet ground state and the lowest triplet excitation of a single Heisenberg plaquette. A hard-core constraint restricts the boson occupation number of each plaquette $s^\dagger s + \sum_\alpha t_\alpha^\dagger t_\alpha = 1$ so that the bosonic representation obeys the spin algebra. The energy of a single plaquette becomes $\mathcal{H}_P = E_s s^\dagger s + E_t \sum_\alpha t_\alpha^\dagger t_\alpha$. Following the standard procedure,^{3,18,19} we obtain a triplet mode with dispersion (in units of $J_1 = 1$)

$$\omega^2(\mathbf{k}) = J'^2 + \frac{2}{3} J' [(1 - 2J') \cos k_x + (J_2 - 2J') \cos k_y]. \quad (3)$$

For $J' > \frac{1}{2} J_1$ and $J_2 < 2J'$ the minimum of the spectrum is at $\mathbf{k} = 0$ and this becomes soft along the line $J_2 = -1 + \frac{5}{2} J'$, which corresponds to the Néel ordering. The first-order

transition line between the dimer and the plaquette phase is obtained by comparing the exact dimer energy with that of the plaquette state including the zero-point motion from the quadratic terms. These lines are depicted as red lines in Fig. 2. The stability region is shifted to larger J'/J , as already observed for the standard SS model, but the slopes are in good agreement with ED. Note that the first-order boundary between the plaquette and the Haldane phase cannot be found with our method since we do not have an expression for the ground-state energy of the Haldane phase.

Conclusion. We have introduced a variant of the SS model with two types of diagonal couplings as a minimal model for the loss of the C_4 symmetry in $\text{SrCu}_2(\text{BO}_3)_2$ under high pressure. We find a quasi-1D Haldane phase where the low-energy physics can be described in terms of fully frustrated decoupled two-leg ladders which form $S = 1$ entities on their rungs. When J_2/J_1 decreases, the gap to the first excitation first decreases linearly, and then levels off after crossing the boundary between the exact dimer phase and the Haldane phase. Assuming that the main effect of pressure is to reduce the ratio J_2/J_1 , this is precisely what has been reported by INS,⁶ as well as by NMR²⁰ for the nonmagnetic sites. However, the presence of magnetic sites possibly arranged on every second ladder, as suggested by NMR,⁵ and of a low-lying excitation below the excitation that levels off, as revealed by INS,⁶ goes beyond the prediction of the present model and requires further investigation.

We would like to thank A. Läuchli, H. M. Rønnow, M. Zayed, C. Ruegg, M. Takigawa, S. Wessel, and K. Penc for fruitful discussions. This work has been supported by the Swiss National Fund and by MaNEP.

*Marion.Moliner@kit.edu

†rousoscha@pks.mpg.de

‡Frederic.Mila@epfl.ch

¹S. Miyahara and K. Ueda, *J. Phys. Condens. Matter* **15**, R327 (2003).

²A. Koga and N. Kawakami, *Phys. Rev. Lett.* **84**, 4461 (2000).

³A. Läuchli, S. Wessel, and M. Sigrist, *Phys. Rev. B* **66**, 014401 (2002).

⁴M. Takigawa, T. Waki, M. Horvatić, and C. Berthier, *J. Phys. Soc. Jpn.* **79**, 011005 (2010).

⁵T. Waki, *J. Phys. Soc. Jpn.* **76**, 073710 (2007).

⁶M. Zayed *et al.* (private communication).

⁷H. Kageyama *et al.*, *Physica B* **329-333**, 1020 (2003).

⁸A. Honecker, F. Mila, and M. Troyer, *Eur. Phys. J. B* **15**, 227 (2000).

⁹N. B. Ivanov and J. Richter, *Phys. Lett. A* **232**, 308 (1997).

¹⁰I. Bose and S. Gayen, *Phys. Rev. B* **48**, 10653 (1993).

¹¹F. D. M. Haldane, *Phys. Rev. Lett.* **50**, 1153 (1983).

¹²Up to third order, the effective ladder couplings are $J_R = J_2 - J'^2/J_1 - \frac{1}{2} J'^3/J_1^2$ and $J_L = J_x = \frac{1}{2} J'^2/J_1 + \frac{3}{4} J'^3/J_1^2$.

¹³Site 0 couples to sites 6 and 10 through J'^3/J_1^2 and to sites 7, 9, 11, and 12 through $\frac{1}{2} J'^3/J_1^2$. Site 0 is also coupled to site 8 belonging to the next-nearest-neighbor ladder through J'^3/J_1^2 .

¹⁴We note here that a triplon excitation prefers to sit on the J_2 bonds since $J_2 < J_1$.

¹⁵For the Néel boundary $J'_c(J_2)$ of Fig. 2 we made an unbiased search from all clusters with 16, 20, 24, 28, and 32 sites. Using the most symmetric clusters (16 and 32 sites) shifts J'_c by no more than a few percent.

¹⁶C. Knetter, A. Bühler, E. Müller-Hartmann, and G. S. Uhrig, *Phys. Rev. Lett.* **85**, 3958 (2000).

¹⁷S. Sachdev and R. N. Bhatt, *Phys. Rev. B* **41**, 9323 (1990).

¹⁸M. E. Zhitomirsky and K. Ueda, *Phys. Rev. B* **54**, 9007 (1996).

¹⁹O. A. Starykh, A. Furusaki, and L. Balents, *Phys. Rev. B* **72**, 094416 (2005).

²⁰M. Takigawa *et al.* (private communication).